

## CHAPTER 4

# RESEARCH EQUIPMENT, INSTRUMENTATION AND CALIBRATION

Two instrumented research equipment were developed to measure the required parameters for the realisation of the objectives of this study. The first equipment was the instrumented experimental deep rotavator while the second was an instrumented apparatus for the *in situ* measurement of the soil strength and soil-metal friction parameters. The equipment was mounted on separate tool-frame carriers that were hitched onto separate tractors. The two tool-frame carriers were equipped with appropriate hydraulic systems for controlling their heights during the field trials and transportation, and to operate the soil strength characterisation apparatus. The rotavator was hydraulically driven using a hydraulic motor connected to the tractor PTO shaft. This chapter gives details of the functional components of the research equipment, instrumentation, calibration, and the data acquisition systems (DAS) used to collect the experimental data.

### 4.1 The instrumented experimental deep tilling rotavator

#### 4.1.1 Functional components

A schematic layout of the developed instrumented experimental deep tiling rotavator mounted on the tool-frame carrier is shown in Figure 4.1. The tiller comprised a tool-frame carrier, the deep tilling rotavator, a variable displacement hydraulic pump, a hydraulic motor, and transducers for measuring the desired outputs. The tiller tool-frame carrier was attached to a tractor through the two lower links and the top link of the tractor. The tiller is driven by a constant displacement hydraulic motor (component 9 in Figure 4.1), which is mounted onto the driving shaft of the rotavator. The hydraulic motor is driven by a bi-directional variable displacement hydraulic pump (*Bosch, Germany*, not shown in Figure 4.1), which is connected to the tractor PTO shaft.

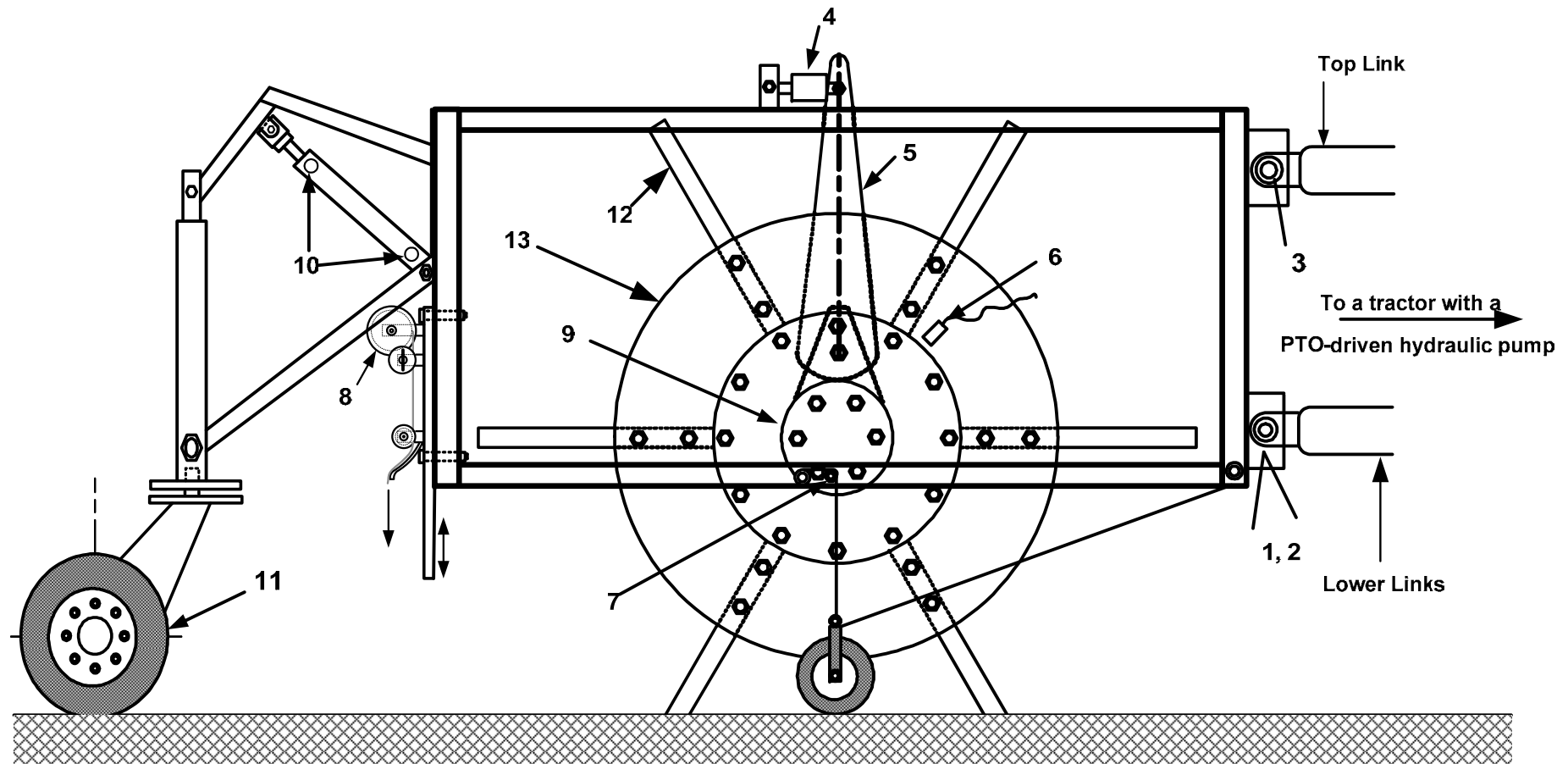


**Figure 4.1:** Side view of the instrumented experimental deep rotavator (1, 2 – lower right and left force transducers; 3 –top link force transducer; 4 – torque load cell; 5 – torque arm; 6 – magnetic proximity detector; 7 – cable-extension displacement potentiometer; 8 – integrated optical transducer for measuring distance travelled; 9 – Hydraulic motor connected to a tractor PTO-driven bi-directional variable displacement hydraulic pump, 10 – double acting hydraulic cylinder for lifting; lowering the rear of the tool-frame carrier and the lifting of the swivel wheel, and 11 – two swivel wheels; 12 – Extension arm; 13 – Flange).

Commercially available standard L-shaped blades were purchased from a local supplier and fitted at the lower end of the extension arms (component 12, Figure 4.1) of the tiller. Such blades give the highest forward thrust forces (Salokhe *et al.*, 1993, Chamen *et al.*, 1979), and should be helpful for deep rotary tillage where increased draft forces are likely to result. The blades were secured at the lower ends of 600 mm long steel extension arms of 80 mm wide by 30 mm thick) using a pair of bolts and nuts. The other end of the extension arms were fixed onto a 16 mm thick circular flange (component 13, Figure 4.1) of 800 mm diameter

The design of the experimental tiller allowed for the easy removal and fastening of the extension arms; and hence the number of blades. This was necessary for investigating the effect of the number of blades on the performance of the tiller. The tiller tool –frame carrier had a swing gate on its left side which was used to access the flange for removal and fixing of the extensions arms together with the blades.

The oil for the hydraulic pump was contained in an overhead tank fitted with a valve at the base of the tank. The structure carrying the hydraulic oil tank was mounted on the frame of the tractor to which the rotavator tool-frame was connected via the three-point links (Figs. 4.1 & 4.2). The direction of rotation of the motor and hence direction of the tiller blades could be changed by either changing the inlet and outlet oil pipes into the hydraulic motor or by changing direction of the outlet valve on the pump. Both the inlet and outlet hydraulic oil pipes from the pump to the motor were of 37 mm diameter. The excess/leakage oil was returned to the tank via a 25 mm diameter hydraulic pipe from the hydraulic motor.

The tiller tool-frame is supported by a swivel wheel at the rear and the custom-built tractor three-point hitch system at the front. Both the rear and front parts of the tool-frame can be raised and independently lowered using the tractor standard hydraulic system, with the top link removed for transport. For the front, the lift mechanism of the three-point hitch point was used while for the rear, a double-acting hydraulic cylinder (Figure 4.2) connected to a suitable lifting mechanism that rested on top of the swivel wheel. The hydraulic systems for controlling the height of the tiller tool-frame carrier and for driving the hydraulic pumps via the tractor PTO used separate hydraulic circuits.

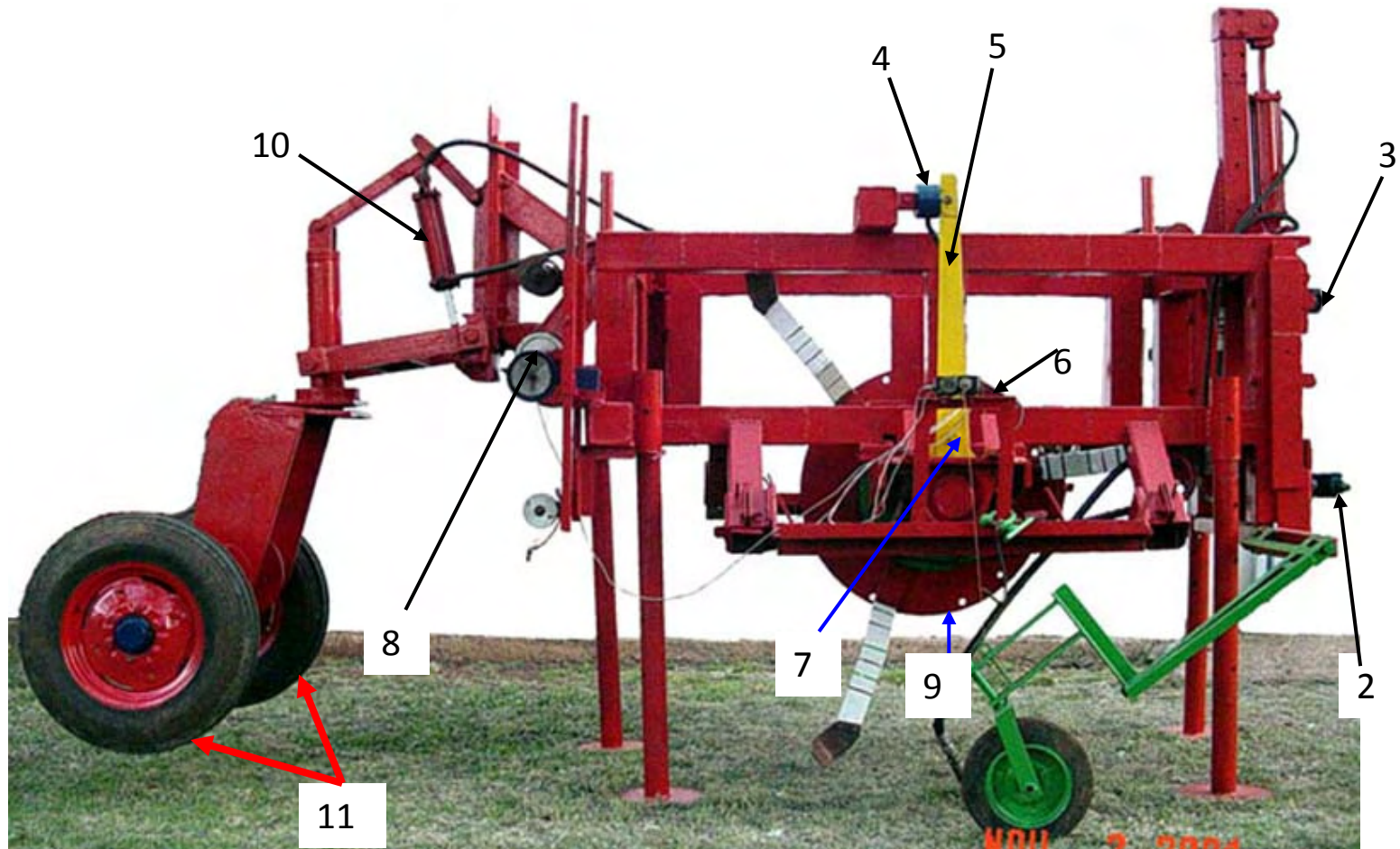


**Figure 4.2:** The fabricated experimental deep rotavators showing some of the key functional components (1- left link force transducer (hidden); 2 – Right lower link force transducer; 3 – top link force transducer; 4 – torque load cell; 5 – torque arm; 6 – magnetic pick-up (hidden); 7 - cable-extension displacement potentiometer; 8 – integrated optical transducer; 9 – hydraulic motor (partly hidden); 10 – double acting cylinder; 11 – swivel wheels)

The tractor hydraulic systems were used to control the height of the tool-frame during transport with the top link removed. For the setting and controlling the depth during the field experiments, the top link was set to a length equal to the length of the two lower links. The equal length of the three links was necessary for keeping the top and lower links parallel during field test. This was done to ensure that only horizontal thrust or pull forces were generated during field tillage experiments. During storage, the rotavator tool-frame was rested on four support legs (Figure 4.2). The support legs were lifted and held in place with metal pins/pegs during field experiments and transportation.

#### **4.1.2 Instrumentation of the experimental deep tilling rotavator**

The complexity of the rotavator tillage process necessitates simultaneous measurement of many variables (Romig, 1971) in order to determine its performance. The instrumentation for the experimental rotavator was designed to measure the horizontal force reactions on the three-point hitch of the tractor and the rotor shaft torque variation during tillage. Additional measurements needed to determine the performance of the tiller included the rotor rotational speed, the forward tractor travel speed, the tillage depth, and the soil condition.

The torque applied by the hydraulic motor was measured using a tension/compression load cell of nominal load rating of 2.5kN. The load cell (component 4, Figures 4.1 and 4.2) was connected to an 800 mm long torque arm (component 5). Thrust or pull forces generated was measured by the purpose made strain gauge force transducers connected to the three point hitch system of a tractor (Figure 4.2). Each of the three links had a calibrated force transducer to measure force components in the horizontal directions. The resultant push or pull was the summation of the forces experienced at the two lower links and the top link. The strain gauge force transducers had a nominal force rating of 10 kN (du Plessis, 2004).

The strain gauges for force transduction were bonded (Figure 4.3c) onto a 30 mm square section made of special stainless steel of 1500 MPa yield stress (du Plessis, 2004). The square steel section with the bonded strain gauges was fixed onto the tool-frame carrier



at one end. The free end had of the force transducer had a provision for attaching the links of the three-point tractor hitch system (Figures 4.3b and 4.3c).

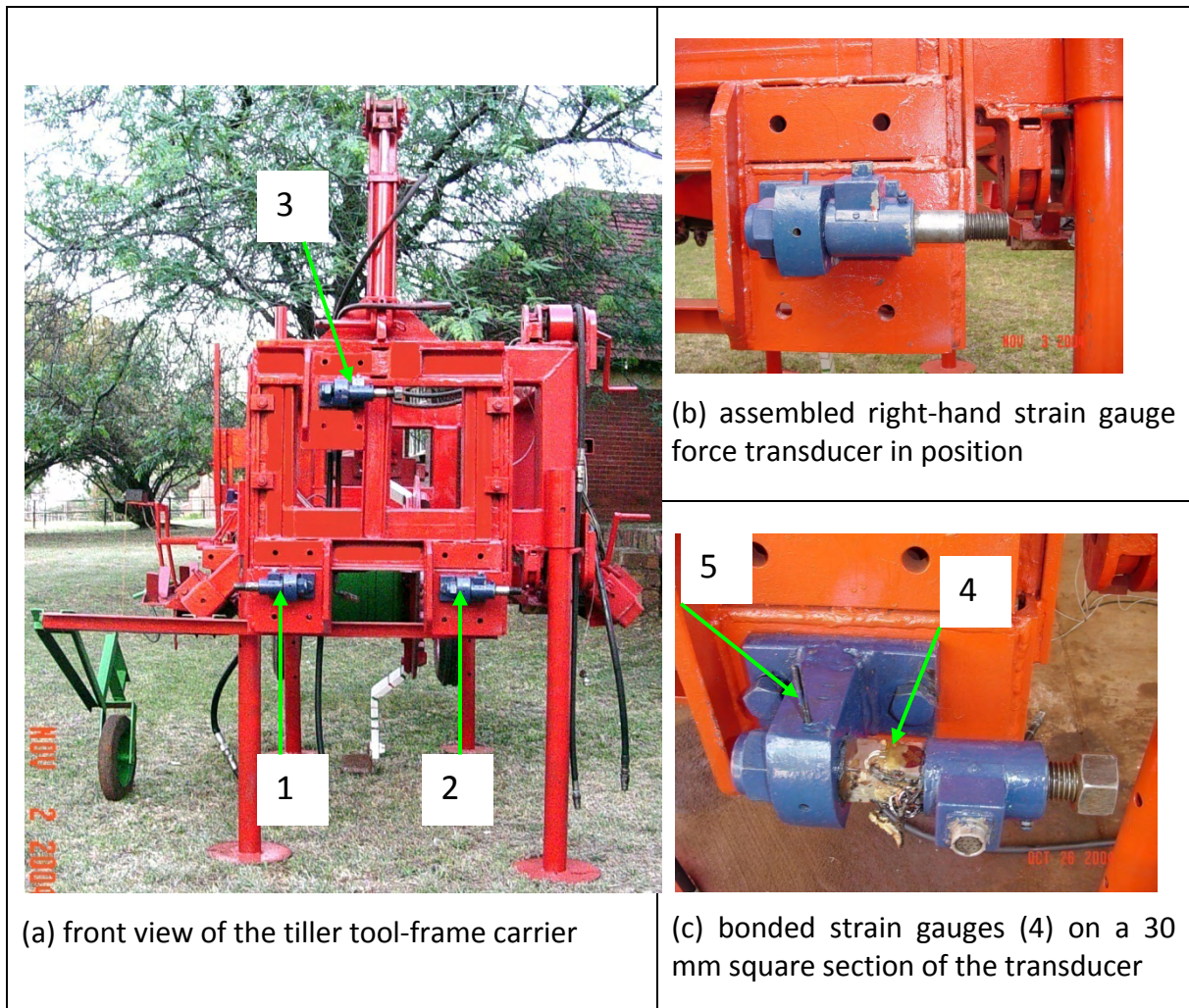


**Figure 4.3:** The strain gauge force transducers (1, 2 & 3 - strain gauge force transducers; 4 – bonded strain gauge; 5 – restraining pin)

The assembled force transducer formed a ‘cantilever-like’ beam when fastened onto the tool-frame (Figure 4.3a). The force transducer comprised two identical strain gauges, one on top and the other at the bottom surfaces of 30 mm square made from special steel (du Plessis, 2004). The strain gauges were fixed (bonded) on these surfaces at 45° (Figure 4.4). With this arrangement of strain gauges, the transducer measured the magnitude of shear forces caused by a push or a pull by a tractor link arm at the free end of the cantilever beam assembly. A straining pin (Figure 4.3b) was used to lock the square steel section in position to ensure that only the horizontal forces were measured.

Depth of tillage was measured as the vertical distance between the soil surface and the lower point of the tip of the blade. The tiller tool-frame depth setting was constrained by the two hydraulic systems used to lower and raise it to the desired depth of operation. The depth measurement transducer was a string-driven ten (10) turn 20-k $\Omega$  cable-extension displacement potentiometer (Doebelin, 2004). This depth measurement system could measure up to depth of 1000 mm without appreciable loss of accuracy, which was well beyond the intended experimental tiller's maximum operational depth of 500 mm. Figure 4.4 shows the layout of the transducer used for measuring the depth.

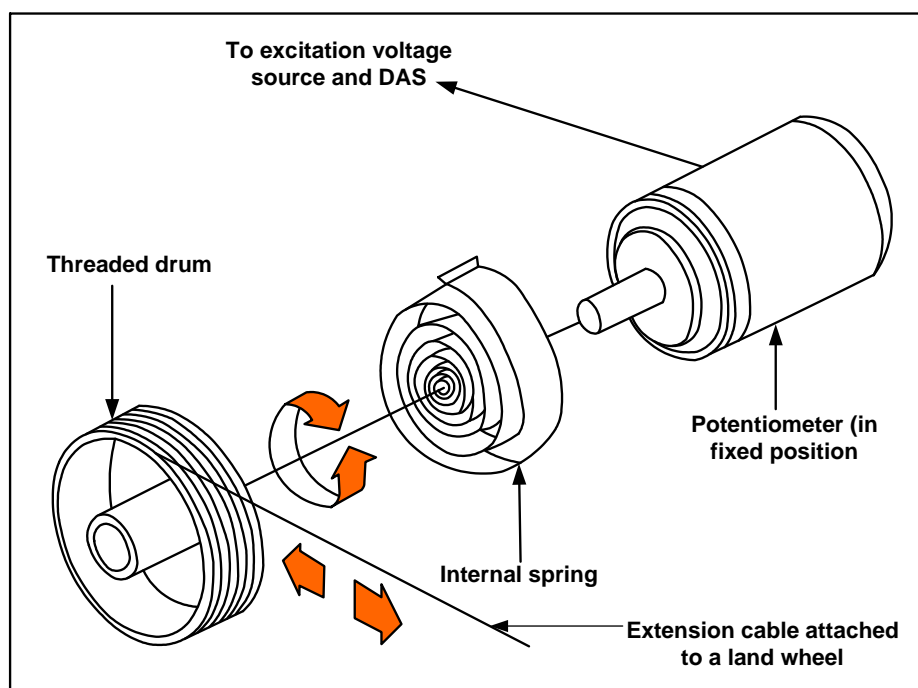


**Figure 4.4:** An illustration of a 20 k $\Omega$  ten-turn cable-extension potentiometer transducer used for measuring the depth of tillage

Rotational speed of the tiller was measured using a proximity magnetic probe. The proximity probe was mounted at an appropriate position on the tiller tool-frame carrier using a flat steel piece extension with a provision for varying the proximity of the probe from the toothed-gear part of the drum housing of the hydraulic motor (Figure 4.5). As the drum rotated the probe generated square wave pulses, corresponding to the crest and trough parts of the geared wheel. The geared wheel fixed onto the rotor drum had 154 teeth and therefore, a complete revolution of the drum generated 154 square-wave pulses.

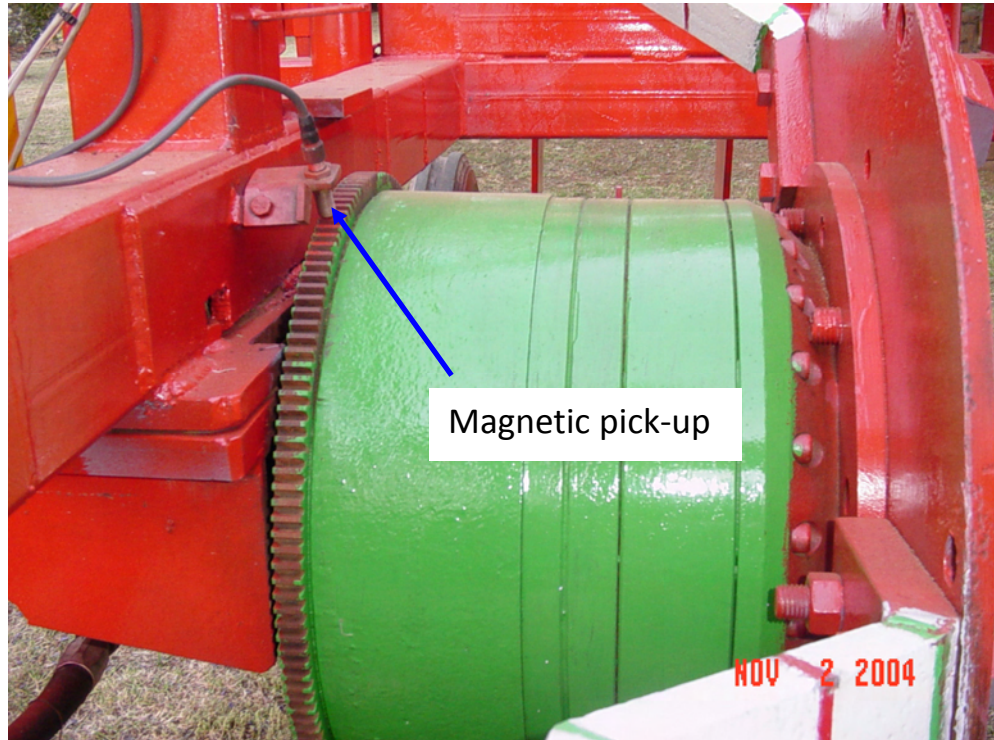


**Figure 4.5:** The magnetic pick-up proximity probe for the measurement of the rotor speed and the angle turned by the rotor

The true ground speed was measured using an integrated optical sensor mechanism (Figure 4.6). The mechanism was connected to a wire rope (component B, Figure 4.6a). As the tractor travelled forward the tension in the wire rope wound around the rubberised section (component C, Figure 4.6) forced the geared wheel to rotate and in turn drove an integrated optical sensor comprising an enclosed probe (component A, Figure 4.6). The rotation caused the generation of square-wave pulses similar to that generated by the rotor speed proximity probe. The wire had a weight with a provision for inserting a peg to hold it firmly into position on the ground during field trials. The system could measure to the nearest  $5 \times 10^{-3}$  m.

The designed travel speed measurement systems measured the distance covered in a given time interval. The forward travel speed of was determined using the standard distance-speed-time relation. Time measurement was done using the in-built PC clock and the DAS software program (§ 4.3). The travel time was predetermined and set for a known duration before measurements were started. All the measurements for the experimental tiller were then done during this predetermined time interval.



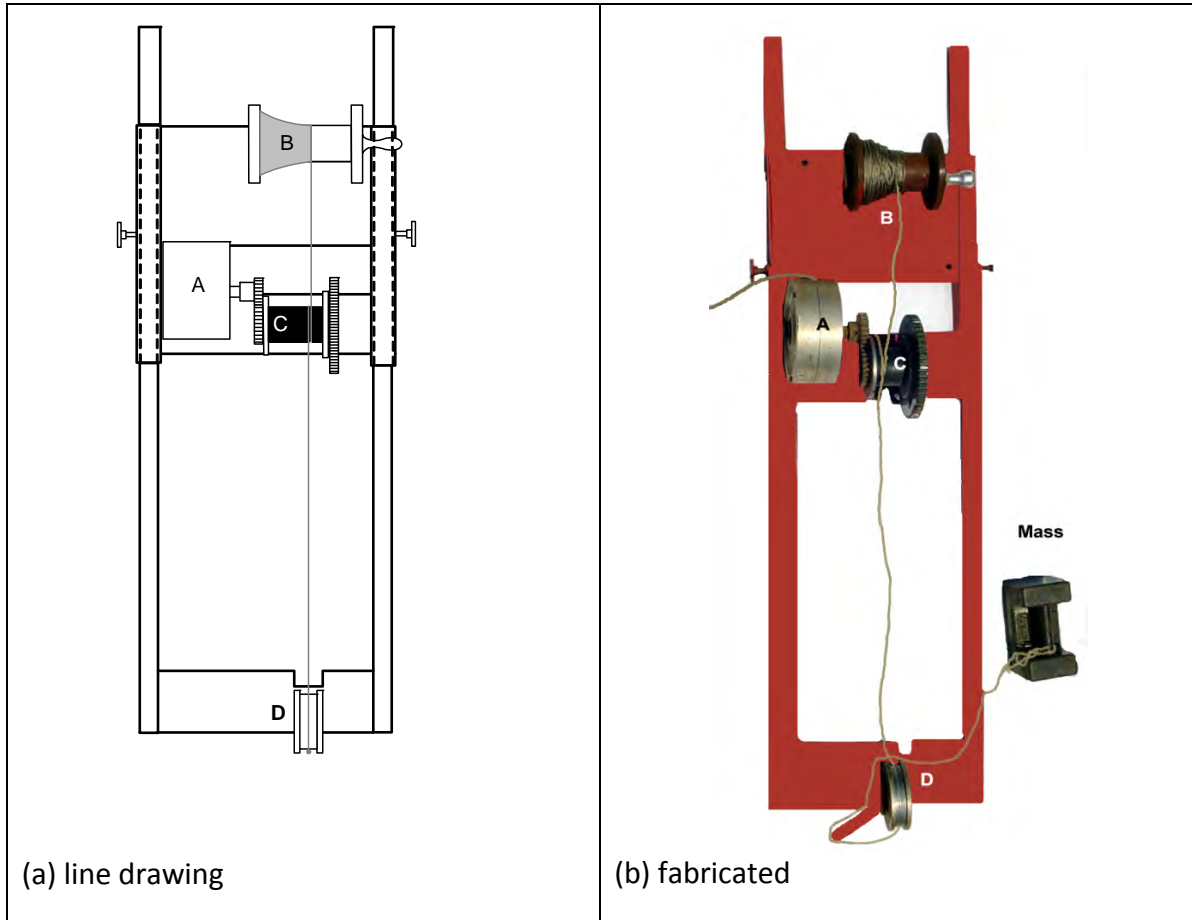


**Figure 4.6:** The assembled ground distance measurement system showing its various components ( A – gearing mechanism with an enclosed integrated optical sensor; B – wire rope wound on a braked drum ; C – rubberised surface on a geared wheel for driving A ; D – wire rope guide)

## 4.2 Soil characterisation apparatus

### 4.2.1 Functional components

Much apparatus and many techniques have been developed and tested for the *in situ* quantification of the soil strength and soil frictional characteristics (Johnson *et al.*, 1987; McKyes, 1989). These *in situ* apparatus and techniques are primarily based on the method of measuring failure by shear in the soil (Johnson *et al.*, 1987). In tillage studies, the use of a particular apparatus depends on its convenience and practical utility with respect to the soil condition(s), and the desired purpose of the soil strength data (McKyes, 1989).

After carefully considering the suitability of the devices that have been used for determining the strength of agricultural soils, the torsional shearing device (Schjønning, 1986; Olsen, 1984) was chosen for this study. The choice of the torsional device was influenced by the need for the determination of soil strength parameters at various depths within the 500 mm depth tilled by the experimental rotavator. Further, it was necessary that the same device be used for the determination of the frictional soil/steel parameters at the same depth as that at which the soil shear strength had been determined. These requirements were satisfied by the versatility of a torsional shear device, as its design would allow easy swapping of heads for measuring the soil shear strength and the soil/steel frictional parameters.

The torsional device designed had two load sensing transducers comprising a torque arm force strain gauge transducer and an industrial load cell (Figure 4.7). The load cell was used for recording the applied normal loads while the strain gauge force transducer was used for measuring the applied torque loads.

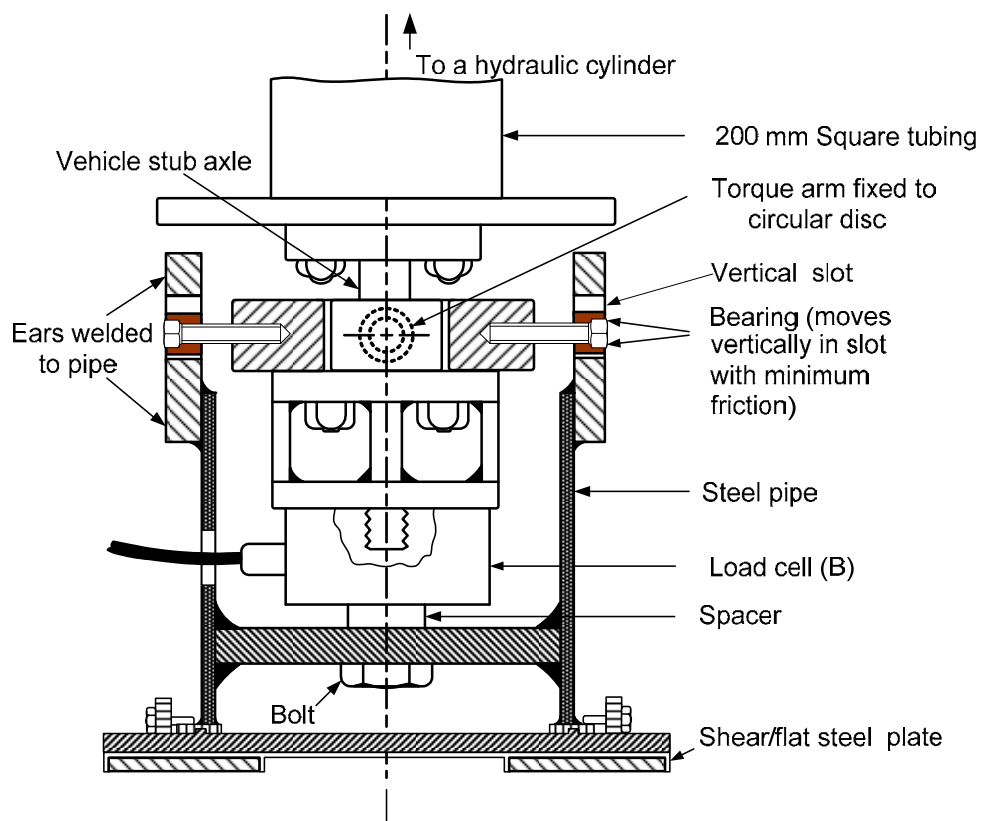


**Figure 4.7:** Cross-section of the torsional shearing device for the determination of the soil shear strength and soil/steel frictional parameters

Two heads (Figure 4.8a and Figure 4.8b), comprising an annulus head with grousers and other a flat polished circular steel plate annulus, both of internal and external diameters of 130 mm and 300 mm, respectively, were fabricated with suitable attachment mechanism. The annulus with grousers head was used to determine the cohesion and angle of internal friction of the soil at various depths.

For the determination of the steel/soil frictional characteristics, the grousers circular annulus head was replaced with the polished circular flat steel plate made from the same material as that of the grousers head. The surfaces of the two heads, which came in contact with the soil during the determination of the soil strength parameters, are shown in Figures 4.8b and 4.8c.

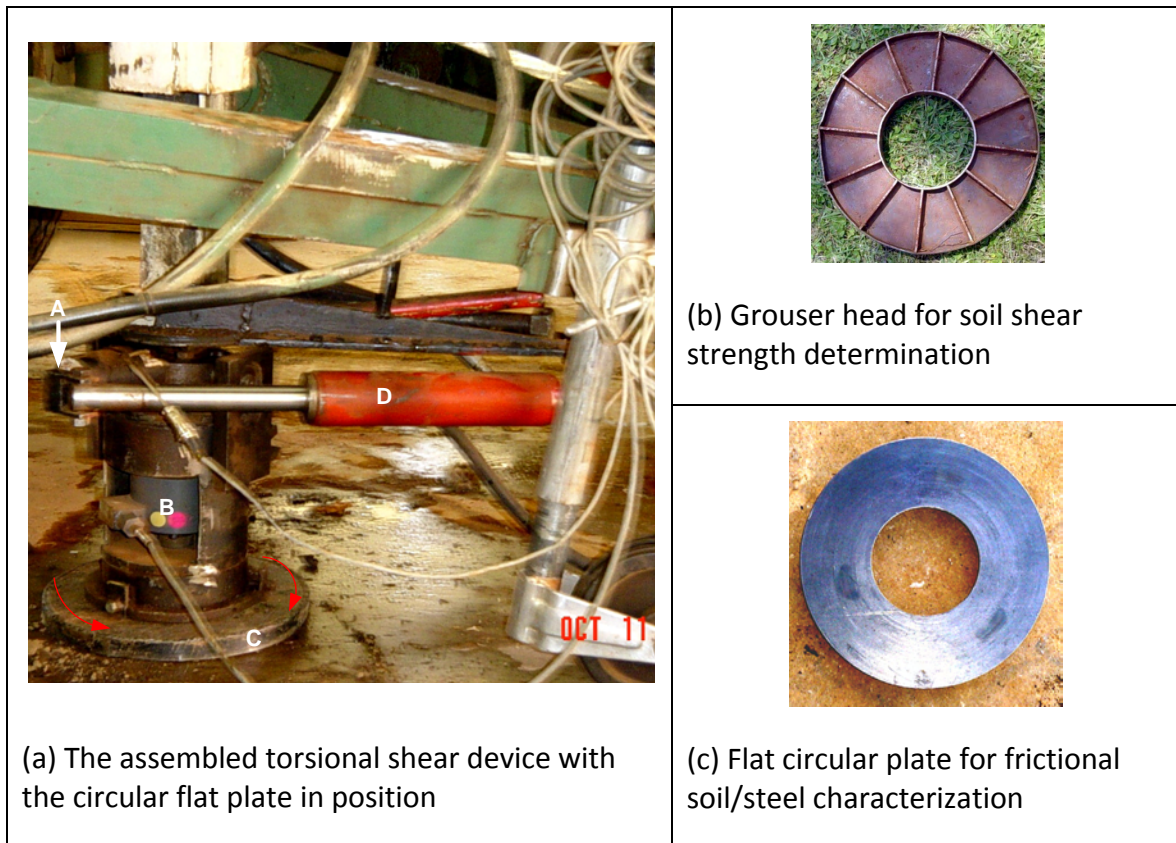


**Figure 4.8:** The fabricated torsional shearing device for determination of soil shear strength and soil-steel frictional parameters (A – torque arm; B –normal/vertical load measuring load-cell; C – grouser head; D – double acting hydraulic cylinder)

To determine the soil strength parameters a normal load and a torque load were applied hydraulically to the torsional shear apparatus. The normal load was measured using a

load cell of 2.5kN nominal rating and the torque load measured using a purpose made strain gauge force transducer connected to the stub axle torque arm (Figure 4.7a). For the application of normal load, an engine operated hydraulic pump (*Robin EH17-20, Fuji Heavy Industries, Tokyo, Japan*) connected to a double-acting hydraulic cylinder was used to apply the load. The magnitude of the load was controlled hydraulically by operating the engine at a constant speed of 4000 rpm by operating the engine at it full throttle, and a given level of opening of the pressure release valve (component C, Figure 4.9). With this set-up, the greater the pre-stress on the control spring, the greater was the normal load applied and vice-versa. During sinkage the vertical load was held constant.

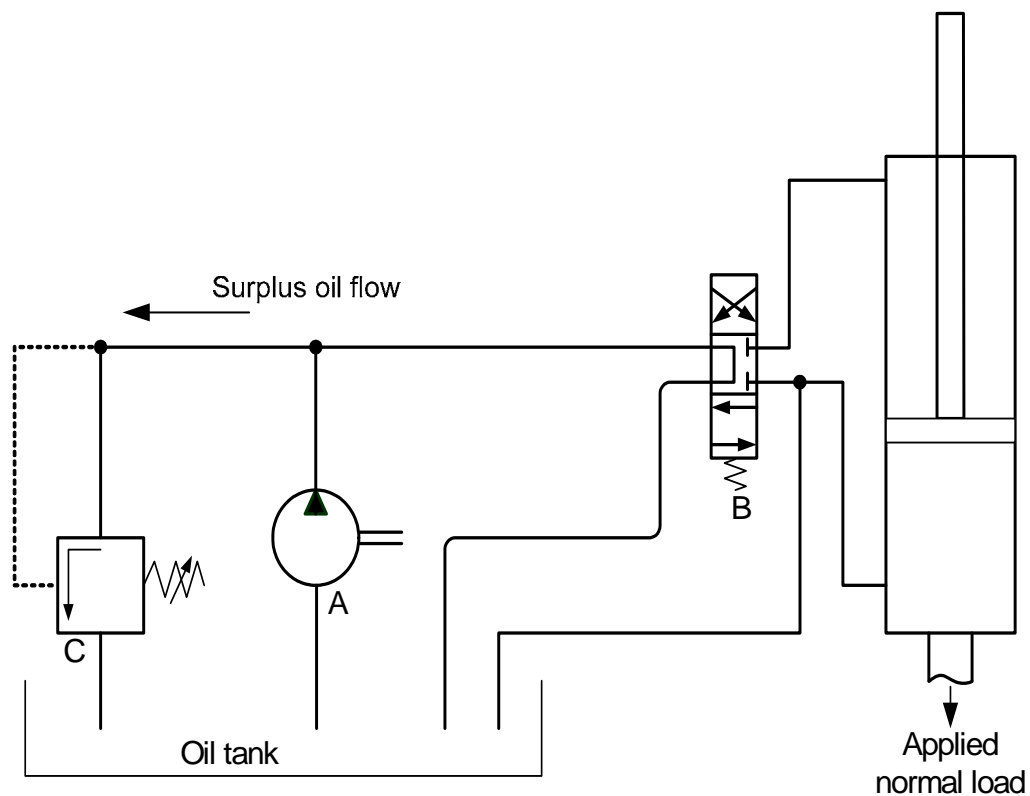


**Figure 4.9:** The special hydraulic circuit for maintaining a constant normal load for the soil shear and frictional shear strength measurement apparatus during sinkage (A – engine driven pump; B – directional control valve; C – flow and pressure control valve with surplus oil back to tank; D – double acting hydraulic cylinder)

The torque load for rotating the head (grouser or friction plate) was applied using the tractor hydraulic system to prevent the interaction between the two hydraulic circuits.



The load was applied slowly by either lifting or lowering the tractor hydraulic control lever thereby inducing the torque hydraulically. Lifting or lowering the hydraulic lever to shear the soil or overcome the soil-metal friction was continued until the stroke of the hydraulic cylinder was completed. During the initial field trials, it was observed that it was easier to apply the load by lowering rather than by lifting the hydraulic lever.

#### **4.2.2 Instrumentation**

The torsional shearing apparatus (§4.2.1) was instrumented so that the normal and the shearing (torque) loads required for the determination of the soil shear strength and soil-metal friction parameters could be measured. The maximum normal load that could be exerted hydraulically by the engine powered pump (Figure 4.9) was about 2kN. The normal load cell was suitably connected to a 200 mm square tubing (Figure 4.7) that was connected to a double acting hydraulic cylinder connected to a special hydraulic circuit (Figure 4.9). The circuit had a pressure control valve for maintaining a certain level of load by restricting the amount of oil flowing back to the reservoir.

The torque load for shearing the soil using the grouser head (Figure 4.8b) or for overcoming the soil-metal friction using the flat circular plate (Figure 4.8c) was applied in the form of a torque through the torque arm (components A and D, Figure 4.8a) using the tractor hydraulic system. The applied torque was measured using a bending arm torque transducers. Depending on the direction of motion of the double-acting hydraulic cylinder, the resultant signal was either negative or positive with respect to the off-set values of the strain gauge force transducer. In order record a meaningful response of the torque load applied, the hydraulic application of the load was done at a slow speed such that on average, the complete stroke length of 0.5m was done in about 45 second.

#### **4.3 The data acquisition system**

Output signals from the two instrumented systems were recorded using appropriate transducers at suitable measurement rates. The signals were fed to a state-of-the-art commercial data acquisition system (DAS), called Spider8 (*Hottinger Baldwin Messtechnik, Germany*), which was connected to a personal computer (Figure 4.10).

The DAS comprised eight (8) input (measurement) channels and a computer software program, called CARTMAN EXPRESS version 3.1, a MS Windows compatible data acquisition program, for reading the measured information from the transducers and storing the data into a file in the PC's hard disk. Each channel of the Spider8 is equipped with a separate A/D converter which allowed data measuring rates from 1 Hz to 9.6 kHz. Using the DAS's in-built clock interface, the experimental measurement periods were set. The in-built clock system was also useful in the determination of both the rotational and forward travel velocities of the rotavator.

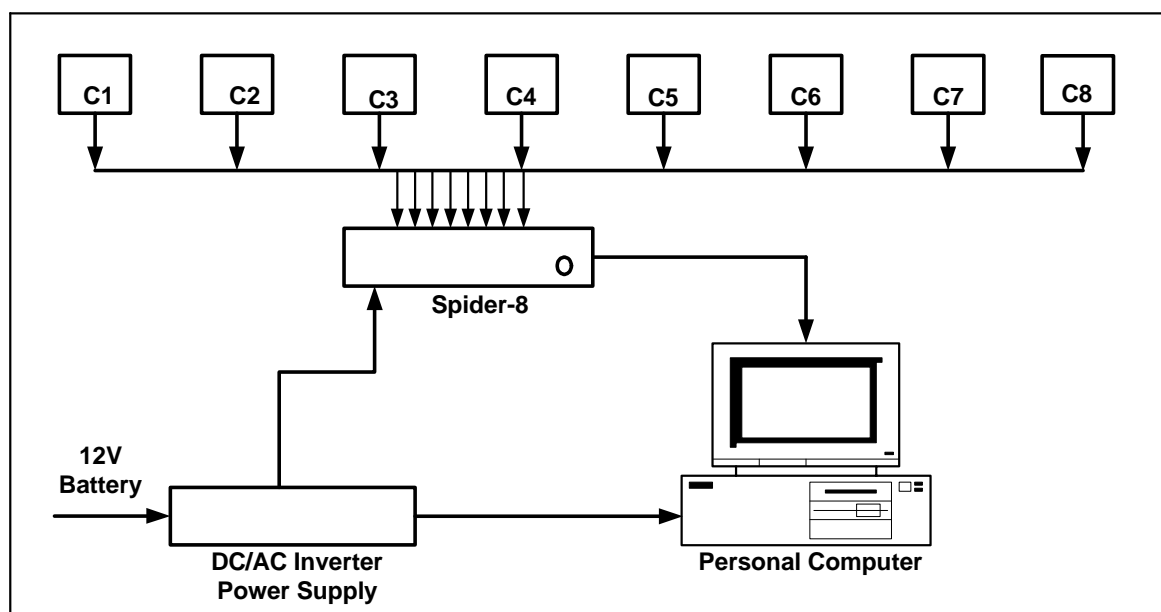


**Figure 4.10:** Schematic diagram of the DAS (C1 ... C8 – measurement channels)

The different transducers for the two research equipment developed; the instrumented experimental deep rotavator and the soil strength characterisation apparatus were connected to the DAS using 15-pin D-type connectors to the various measurement channels (Figure 4.10). The tiller tool-frame had seven (7) transducers comprising three strain gauge force transducers for recording the forces on the two lower links and the top link of the tractor, a load cell connected to the torque arm for measuring the torque, a proximity pick-up sensor for recording the rotational speed of the rotavator, a 20k $\Omega$  ten-turn cable-extension potentiometer displacement transducer (Figure 4.4) for sensing the tillage depth and proximity probe for measuring the tractor forward travel speed. The eighth channel on the DAS was not utilized.

For soil characterization, the torsional shear device utilized two of the eight channels available on the Spider8. Channel 1 was connected to the load cell for measuring the normal load and channel two was connected to the strain gauge force transducer for measuring the torque required to fail the soil through shear or friction overcoming the soil-metal interface friction.

Depending on the type of the transducer connected to a channel, the output signal could be one of voltage for all the force measuring transducers and the depth sensor, or a square-wave (frequency) counter for the all the speed measuring transducers. The DAS was connected to the computer via the parallel printer port and the data measured was stored in the hard disk of the PC in a text file format. Output signals from all the channels were recorded at a predetermined rate, e.g. 2.4 kHz for a preset length of time. Output signals from the channels could be monitored as the measurement progressed using the CARTMAN EXPRESS program. This allowed for easy detection and rectification of faults, and ensured that the correct measurements were made.

## **4.4 Calibration**

### **4.4.1 Calibration of strain-gauge force transducers and load cells**

Force measuring strain gauge transducers and the torque load cell were all calibrated outside the respective tool-frames. Calibration of the strain gauge force transducers was done by fixing them horizontally with the measuring planes vertical and horizontal onto a specially designed beam (Figure 4.11). The fixed strain gauge force transducer and the beam formed a 'cantilever-like' beam, much like the fastening of the transducers onto the tiller tool-frame carrier. Dead loads of known masses, e.g. Figure 4.11, were then hang onto a specially designed metal bar of known mass. The bar was connected to the free end of the fastened force transducer (Figure 4.11).

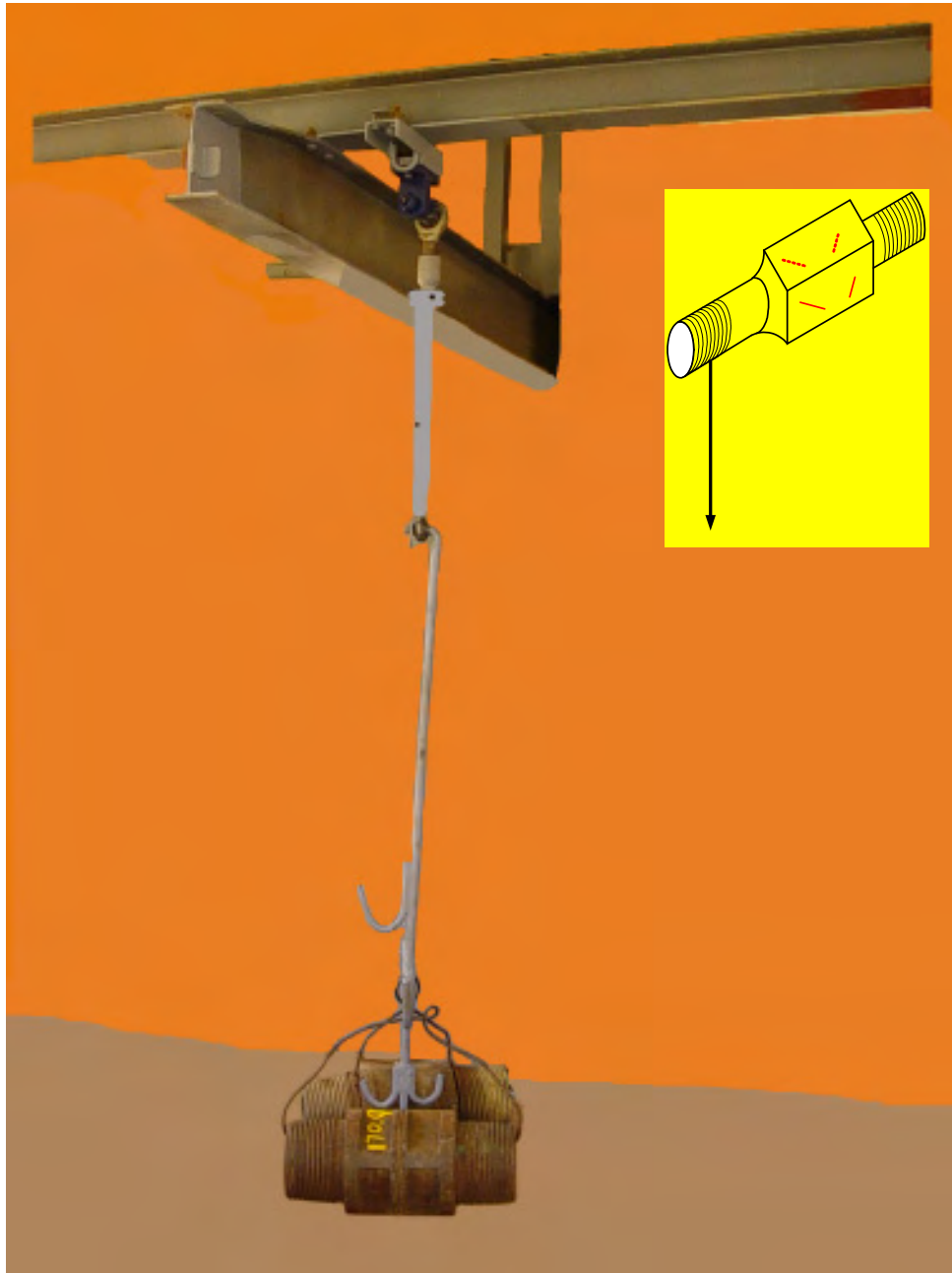


**Figure 4.11:** Calibrating a strain gauge force transducers for one of the tractor links

The loading was continued to a total mass of about 50 % of nominal load capacity of the force strain gauge transducers. For each added mass, a time of about 20 seconds was allowed to elapse before another weight of known mass was added onto the hanging bar. The process was continued until the target weight of hanging weights was reached. The setup was allowed to stabilise after which the weights were removed one-by-one in the reverse loading order, i.e., the last added weight was removed first until all the weights hang on the bar were removed.



A specially designed hanger (Figure 4.12) was used for the calibration of double acting industrial load cells for measuring the torque on the torque arm on the tiller tool-frame carrier and the normal load on the soil strength characterisation apparatus. A load cell that was being calibrated was thereafter placed under a hanging beam and two dead loads of approximately equal masses were placed on either side of the beam and the cam and arm activated to transfer the load to the load cell. Like was the case with the strain gauge forces transducers, the loading was continued to about approximately 50 % of the nominal load capacity of the load cell.

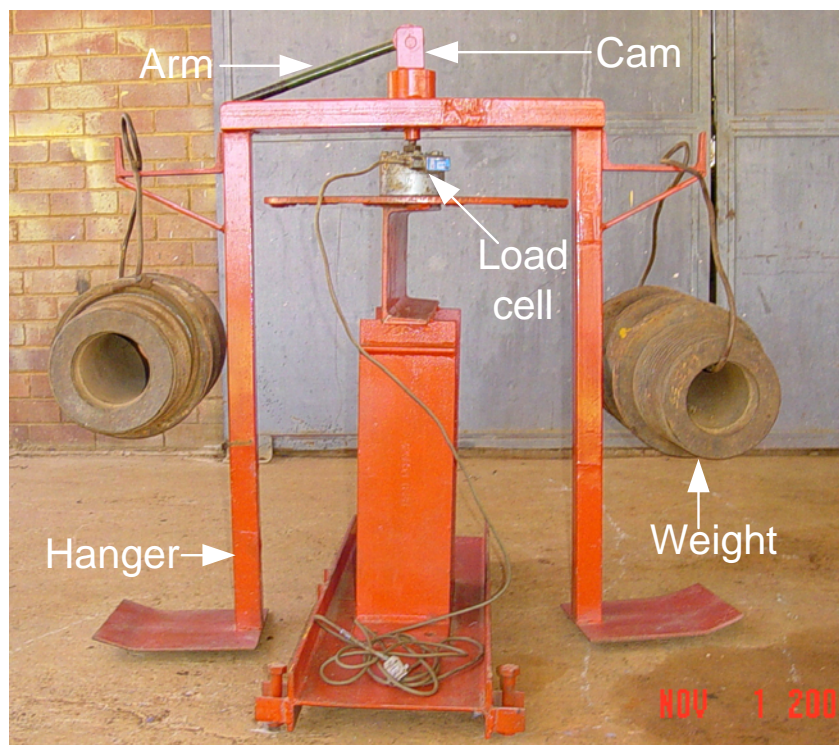


**Figure 4.12:** Calibrating load a cells in compression using a specially designed hanger

At the end of the loading phase a pair of dead loads placed on the hanging beam was removed and the setup allowed to stabilise before the next pair of weights was removed. The unloading phase was done until all the dead loads were removed. The object of this unloading was to counter-check the magnitude of the voltage response of the force transducers at equal loading levels so as to determine the status of hysteresis<sup>2</sup>

---

<sup>2</sup> The difference the in output signal for a given input during loading and unloading phases (Bentley, 1995)

of the transducers. Figure 4.13 is a typical plot of the output signal, done in MATLAB graphics mode, for the calibration of the load cells and the strain gauge force transducers. Similar plots were obtained for all the load cells and strain gauge transducers.

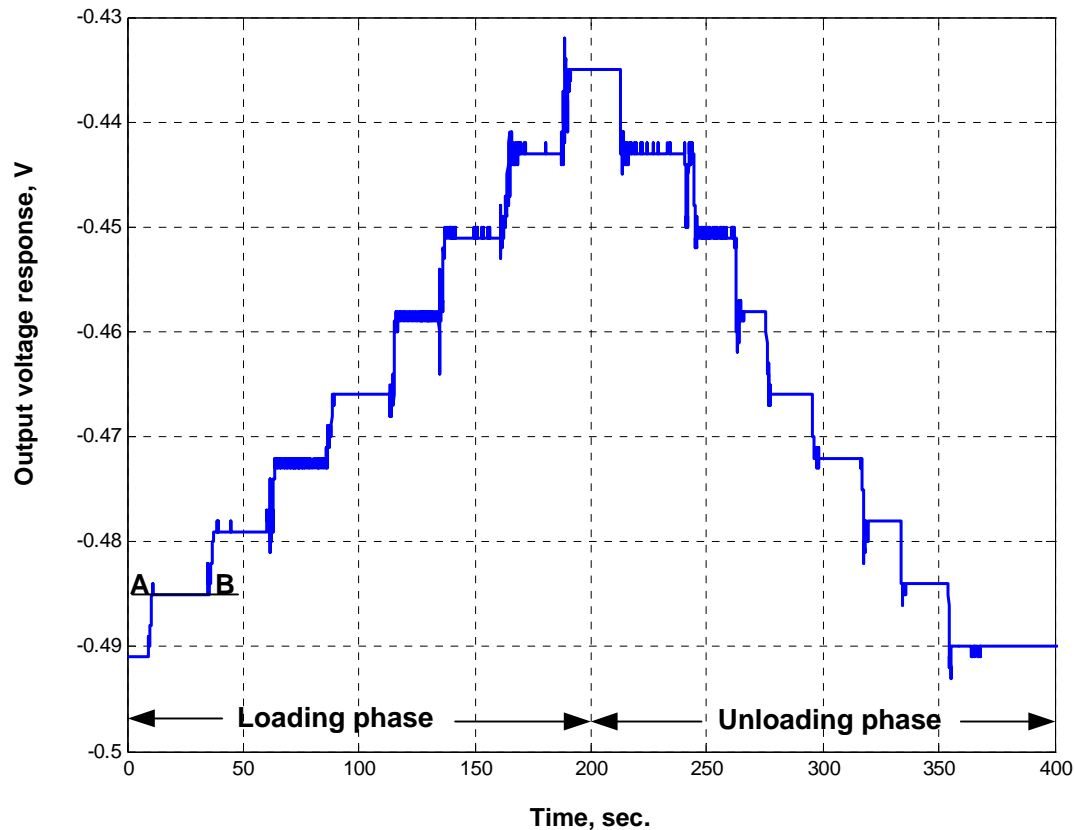


**Figure 4.13:** Typical calibration output signal for strain gauge force transducers and load cell for the loading and unloading phases

In Figure 4.13, the flat portions such 'A-B' which represent constant voltage levels on the voltage axis indicate the total weight registered by the force strain gauge transducers or the load cells with the passage of time of the transducer being calibrated after addition or removal of a dead load. During the loading phase, the voltage response of the load cells or strain gauge force transducer rises in a '*climbing-up staircase manner*' while during the unloading phase, the voltage response curve falls in a '*climbing-down staircase manner*'. In the case of Figure 4.13 the loading phase lasted about 200 seconds, and a total of 8 known dead loads of approximately equal masses were suspended on the load cell or strain gauge force transducer. The loads were then removed, one at a

time (unloading phase, Figure 4.13) and the set-up was allowed to stabilize before removing the next set of weight(s). This was repeated until the all loads were removed. The first and the last constant dead load recorded was the weight of the bar (Figure 4.11) or the hanger (Figure 4.12) for suspending the dead loads. The mass of the rod and the hanger were known.

From plots similar to Figure 4.13, the voltage response values corresponding to known magnitudes of total dead load masses were read of the graph using the MATLAB graphics interactive zoom function. The voltage response was then plotted against the corresponding total dead load weight and the best fit regression line plotted. The resultant regression equation of best-fit lines based on the least-squares technique for all the force and torque transducers was of the form:

$$y = mx + c \quad \dots (4.1)$$

where:

$y$  = voltage response for (V)

$m$  = gradient of the best fit regression line ( $V N^{-1}$  for force or  $VN^{-1}m^{-1}$  for torque)

$c$  = the intercept on the voltage response axis (V)

The best-fit lines were plotted for both the loading and unloading phases of the calibration data. Figures 4.14a and 4.14b are typical best fit lines obtained for a purpose made strain gauge force transducer and an industrial load cell used on the two tool-frame carriers (§4.1 and 4.2).

From plots made and curve fittings results for the transducers, all the regression lines are highly linear with coefficients of determination of 0.99 or greater. The gradients of the fitted regression equations between the voltage response and the applied load were used to determine the calibration factors for the strain gauge force transducers and load cells. Calibration factors determined for load cells and strain gauge force transducers are presented in Table 4.1.

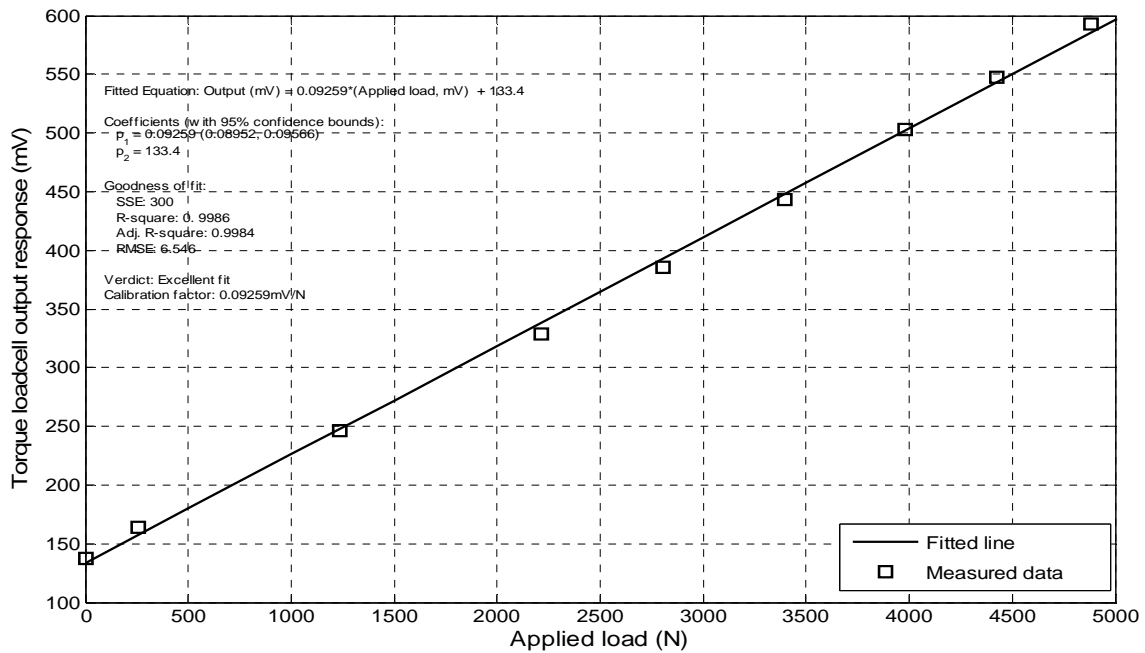


**Figure 4.14a:** Typical loading phase calibration curve for strain gauge force/torque transducers or force/torque load cell; (calibration curve of the strain gauge torque transducer)

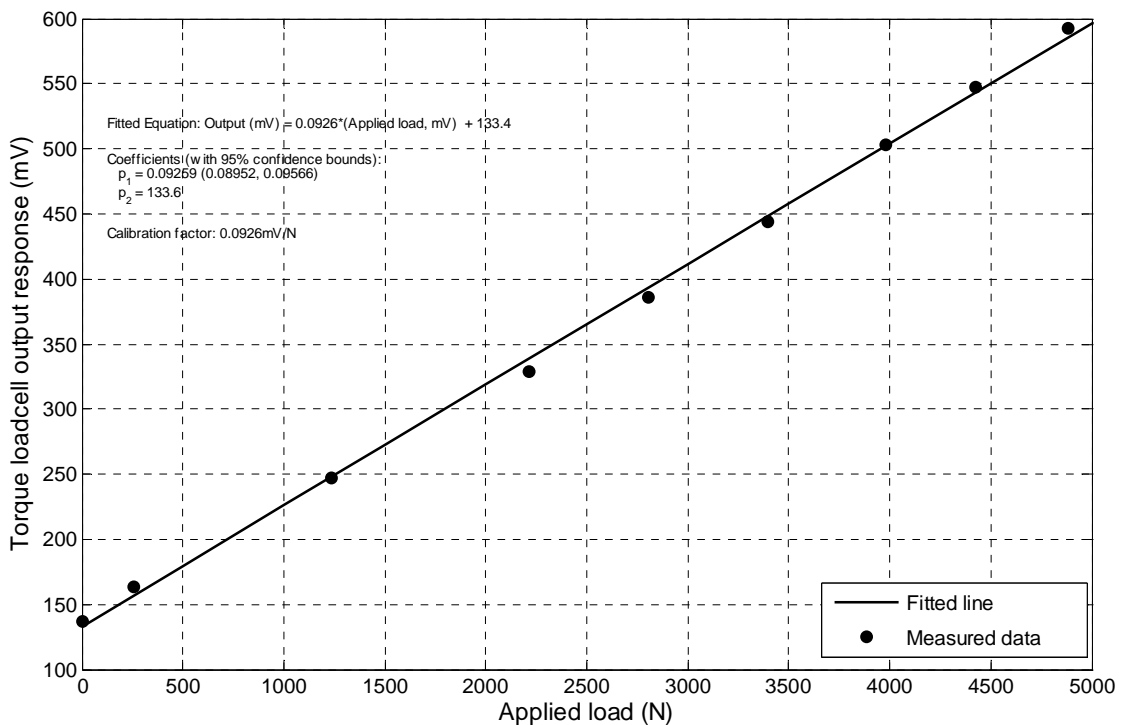


**Figure 4.14b:** Typical unloading phase calibration curve for strain gauge force/torque transducers or force/torque load cell; (calibration curve of the torque arm strain gauge transducer)



**Table 4.1:** Calibration results for the force strain gauge transducers and load cells

Component description	(R <sup>2</sup> )	Calibration factor
<i>Tiller tool-frame force/torque transducers:</i>		
1. Lower left link strain gauge force transducer	0.9999	4.9020 x 10 <sup>4</sup> N/V
2. Lower right link strain gauge force transducer	0.9996	4.4766 x 10 <sup>4</sup> N/V
3. Top link strain gauge force transducer <sup>3</sup>	0.9998	6.3434 x 10 <sup>4</sup> N/V
4. Torque load cell	0.9996	3.7313 x 10 <sup>4</sup> N/V
	0.9999	1.0599 x 10 <sup>4</sup> Nm/V
<i>Torsional shearing device transducers</i>		
1. Load cell for the normal load	0.9999	9.523 x 10 <sup>3</sup> N/V
2. Strain gauge torque transducer	1.0000	407.997 Nm/V

## 4.4.2 Other transducers

### Depth measurement transducer

The twenty–turn 200k $\Omega$  cable-extension potentiometer displacement transducer (Figure 4.4) was used for measuring depth of tillage was calibrated by pulling the string attached through a known distance on a scaled rule and recording the voltage output response using the DAS.

Calibration was done on a flat surface and the string pulled against a scaled metallic rule at 5 mm intervals. The span of calibration was 600 mm, which was beyond the intended depth of tillage operations. A plot of voltage against the distance was made and a regression line of best fit obtained. Figure 4.16 presents the calibration curve for the depth measuring system, together with the calibration factor and the coefficient of determination. The calibration curve is a perfect fit.

### Travel distance and forward speed

Calibration of the travel distance was done in two steps. The first step involved the determination of the number of square waves generated by the sealed proximity probe. Ten complete revolutions were made and the number of pulses generated counted and the average number of revolutions determined. The effective circumference of the

---

<sup>3</sup> New set of strain gauges was fitted for the top link strain gauge force transducer in June 2004 after the initial one with a calibration factor of 6.3434 x 10<sup>4</sup> N/V failed. The bottom calibration factor is for the new top link strain gauge force transducer

section of the geared wheel driven by the wire rope was then determined. The tractor was then driven over known distance and the two distances compared. From the distance travelled, the average speed was obtained using the speed-time-distance relationship.

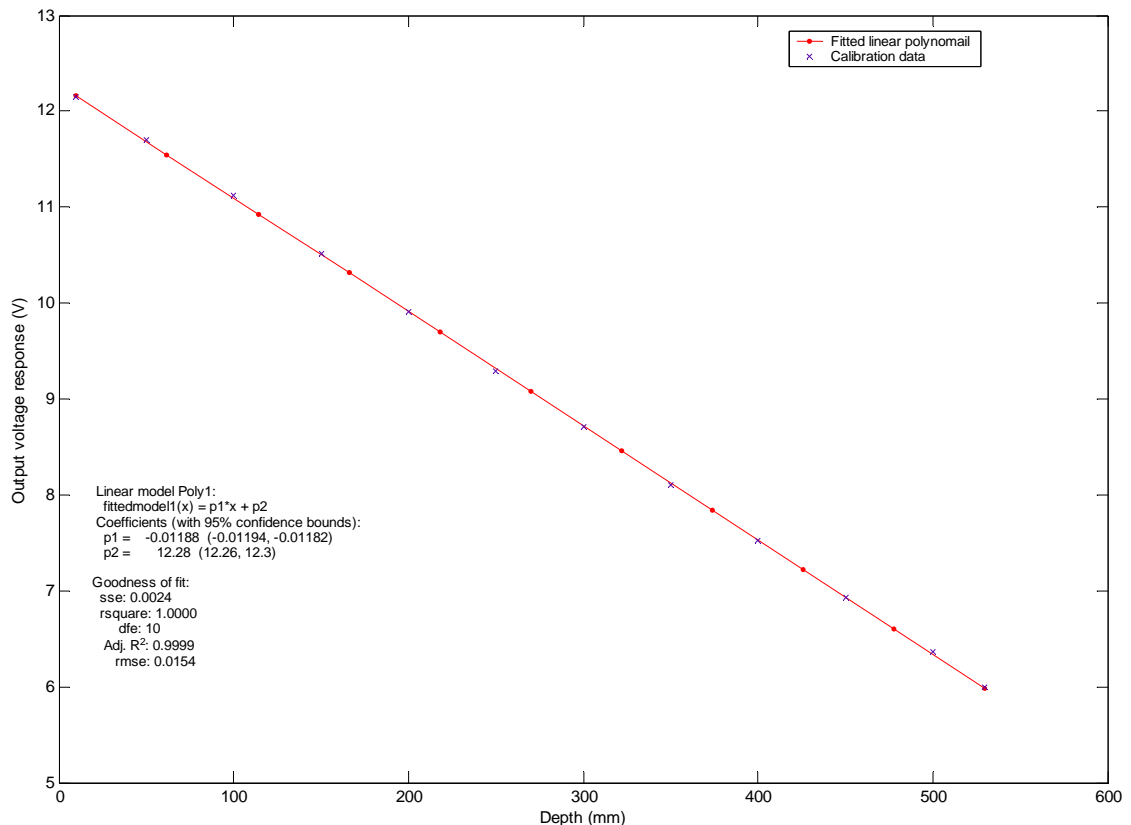


**Figure 4.16:** Calibration curve for the twenty–turn 200kΩ cable-extension potentiometer displacement transducer for monitoring the depth of tillage

### Rotor speed measuring system

Like was the case for the measurement of the distance travelled, the rotor speed was determined using a proximity probe. The number of geared teeth on the drum (Figure 4.5) of the hydraulic motor that rotated at the same speed as the rotor shaft was 154. Thus 154 square waves were generated by the proximity probe for one revolution. The field tests were conducted at a constant tractor engines speed of 2000 rpm. The number of complete revolutions divided by the time taken for doing the tests yielded the rotational speed of the rotor.

## 4.5 Preliminary field testing of the apparatus

Field testing of the apparatus was done in order to determine the operational limitations of the rotavator and the soil shear strength and soil-metal friction characterisation device. The testing was also aimed at determining the data sampling rates, at which the measurements were to be made for the research equipment.

### 4.5.1 The experimental deep tilling rotavator

Measurements for the field testing of the equipment developed were carried out in the field under the intended actual experimental conditions. For the tiller, data was simultaneously recorded at a sampling rate of 2.4 kHz for all the eight channels on the tiller tool-frame carrier. The sampling rate for all the channels was determined by the channel that required the highest rate. In this case the rotor speed measured by the magnetic pick-up channel (4.4) required the highest rate. The in-built clock of the DAS was used for setting the timer over which test-runs was done.

Two tractors, connected by a tow bar, were used during the field testing (Figure 4.17). The use of the two tractors was to eliminate slippage, which would affect the performance of the tiller. The leading tractor provided the draft force for the forward travel only, while the tractor to which the rotavator tool-frame carrier was mounted provided the rotary power through its PTO shaft. Depth was the only operational parameter varied during the field testing. The depth of tillage was varied from 200 mm to 450 mm in steps of 50 mm in order to assess the resultant transducers output response. Field testing was done at a constant rotor speed after setting the engines speed of the two tractors. The forward travel speed maintained constant by operating the towing tractor on one forward travel gear, at a time, at a constant engine speed of 1000 rpm.

At the end of each test run, which was done for a specified length of time, the data was exported by the Spider8 interfacing program (*CARTMAN EXPRESS version 3.1, HBM, Germany*) and stored in the hard disk of the on-board computer. A second program, also developed in MATLAB, was used to determine the number of square-waves generated

by the magnetic proximity probe channel and the integrated optical transducer channel for the determination of the rotor speed and forward travel speed, respectively.



**Figure 4.17:** Setting-up for a tillage test-run [the swivel wheel at the rear end of the rotavator tool-frame carrier was lifted off the ground during tillage experiments]

Graphs of the pull/push forces on the tractor three-point link, the torque requirement and depth of tillage were thereafter plotted while still in the field and a visual inspection of the respective output responses effected. The object of the visual inspection was to ascertain the validity of the recorded transducer outputs. Figure 4.18 is a typical plot of the channel output responses for the three strain gauge force transducers and the input torque transducer.

From Figure 4.18 the portion of the various output response section that are constant, correspond to the measurements recorded taken when the rotavator was stationary for initialising the respective channels. The recording of data with the equipment stationary was necessary for the force and torque measuring channels because the 'zero' load value for these channels formed the basis for determining the magnitudes of the loads recorded during tillage tests.

In Figure 4.8, the sudden change in the response of the occurring at data point  $4.8 \times 10^4$  correspond to the beginning of a test with the rotavator cutting the soil and the towing tractor in forward motion. The part enclosed within the rectangle for data points in the range  $7.0 \times 10^4$  to  $10.0 \times 10^4$  is presented in Figure 4.16, which give a better view of the variation of the response signals from the force strain gauge transducers and the load

cell on the torque arm. It was observed that immediately after the initial jump from the recordings taken when the set-up was stationary to recording taken when doing a trial run, the output response for the force transducer channels maintain fairly constant values. Further, by looking at the direction of this sudden jump, the forces in the two lower links oppose the force in top link during the rotavator operation.

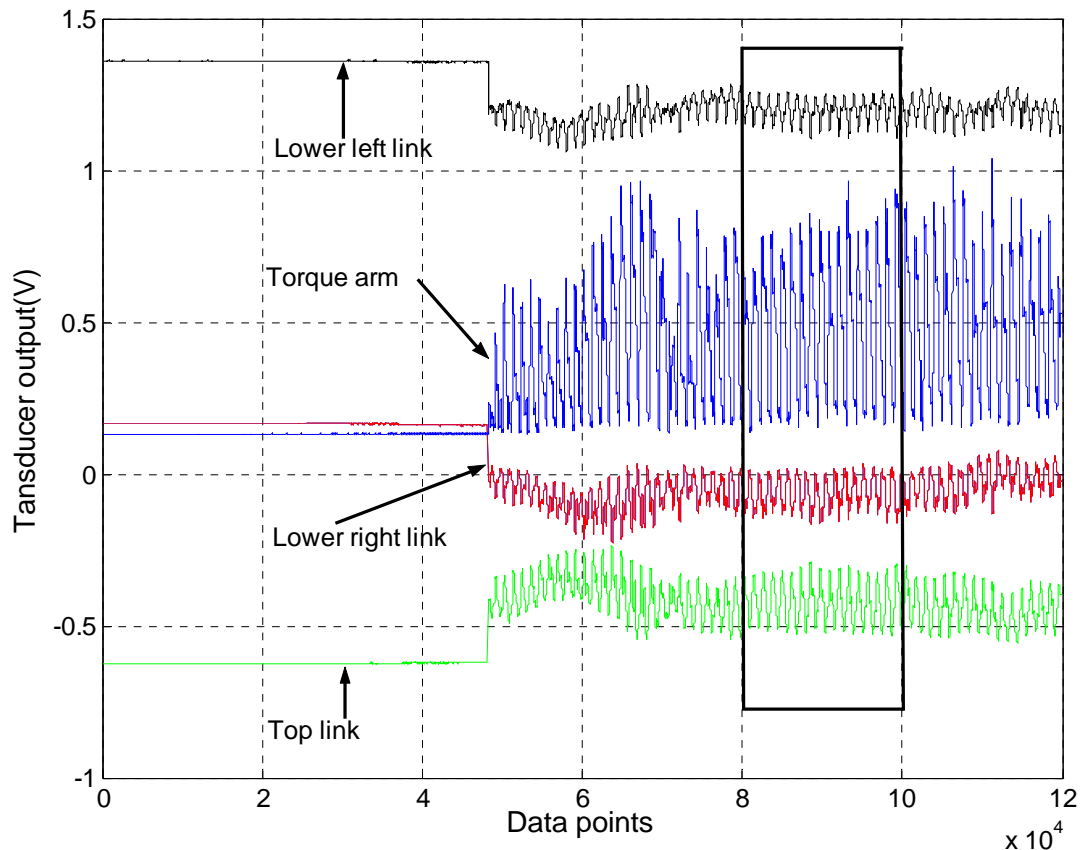


**Figure 4.18:** A typical plot showing the signal outputs obtained for the tiller strain gauge force transducers and the torque load cell during a down-cutting operation

The output responses the forces push/pull forces on the three-point hitch links and the torque on the torque arm are cyclic in nature (Figure 4.19). The torque link response is in phase with the top link phase and out of phase with the pus/pull force in the left and right lower links of three-point hitch system. In general the torque load fluctuate between zero (initialisation values) and a maximum value during down cut tillage while the push pull forces fluctuate within some confined ranges that are significantly different from their initial values. The cyclic nature observed for all channels corresponded to the



cutting actions by individual blades. This was established by plotting the torque response curve against the angular position of the blade from the horizontal.

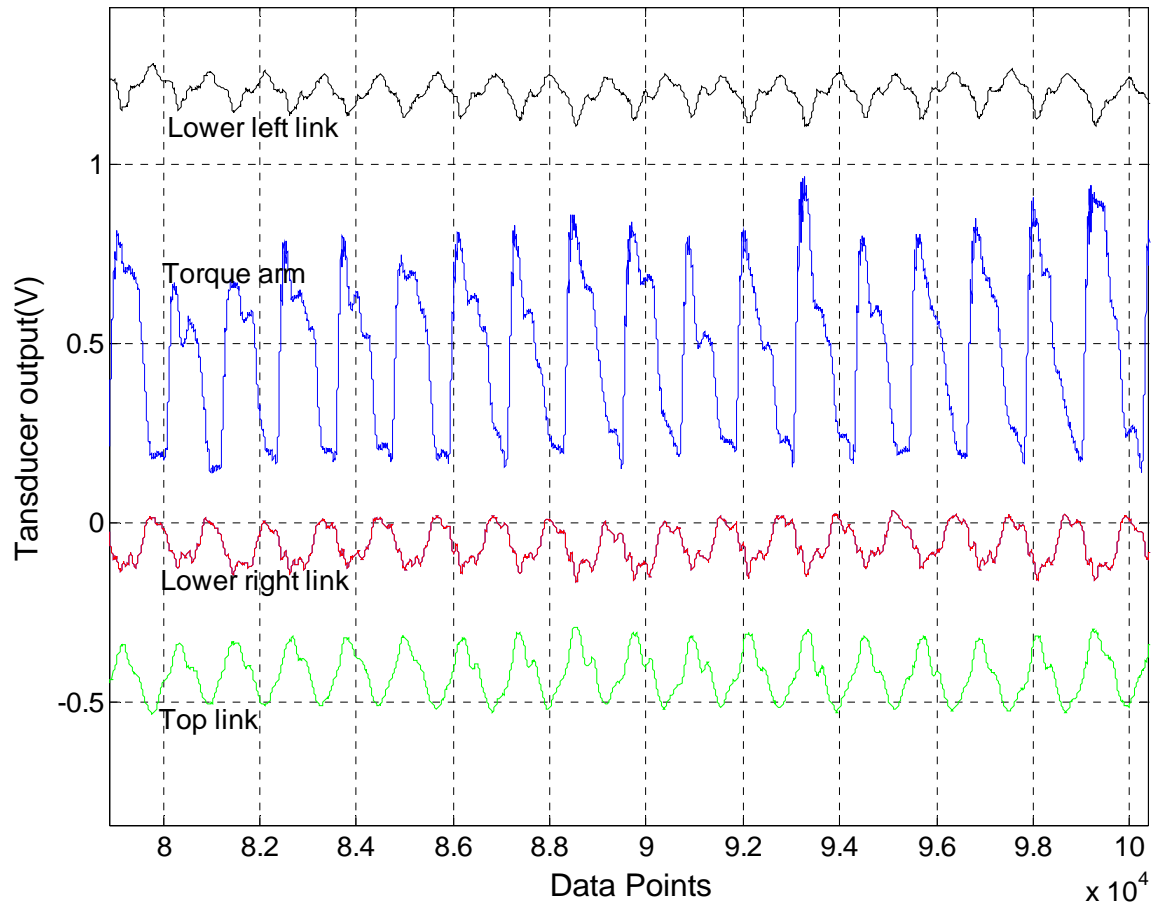


**Figure 4.19:** Expanded view of the output responses of the three point force transducers and the torque load cell for a down-cutting tillage test run

The magnitudes of the applied forces (on the three links), torque and depth of tillage recorded by the respective channels, were calculated using the respective calibration factors (Table 4.1, § 4.4.1) and the following equation.

$$O = CF \times V \quad \dots (4.2)$$

where:

O = magnitude of the applied force (N), torque (Nm) or depth (mm)

CF = calibration factor for the respective transducers

V = the respective voltage output response for a transducer

The rotor rotational speed and the forward travel speed were calculated using another computer program developed in MATLAB. This program also calculated the kinematic parameter,  $\lambda$ , and the bite length,  $L_b$ .

#### **4.5.2 The soil strength characterisation apparatus**

The torsional shear apparatus was field-tested at a data sampling rate of 60 Hz. The purpose of the preliminary field testing of the shearing device was threefold. First, it was necessary to determine the length of time necessary to record for a set of normal load and torque data using the torsional shear apparatus. Second, since the soil strength characterisation was to be determined at different depths, it was also necessary to determine the maximum depth that this apparatus could be operated at under field conditions. Finally, these tests were done in order to ascertain that the output response signals from the normal load and torque transducers were consistent with the expected outputs. The maximum depth that the shear device could reach was 320 mm.

The tests were done on a levelled ground surfaces at a depth of about 10 mm. Only the groused ring head (Figure 4.8b) was used for the preliminary field-testing of the shear device. The decision to use only the groused head at this stage was based on the fact that the procedure for determining of the soil shear strength and the soil-metal friction parameters using this apparatus is based on the same principle (see §4.2.1). During the tests, the desired level of the normal load was set using a digital read-out, connected in series with the load cell for measuring the normal load, via an electrical switch.

Once the normal load was set, the DAS was started and after about 30 seconds, the slow application of the torque load commenced. The torque load was applied for about 60 seconds. The torque load was applied for the full length of the shear device torque load hydraulic cylinder through an angle of about 60°. At the end of a test-run, the voltage output response of the applied normal and torque loads for the shear device were also plotted and visually inspected at the field for every test-run done

A typical plot of the normal and the torque loads voltage output response curves for the shear device is shown in Figure 4.20. Similar output voltage responses were obtained for the grouser head and the flat circular steel plate. Using Equation (4.2), the voltage

responses of the normal and the torque load channels were converted to their normal load and torque equivalents using the respective calibration factors given in Table 4.1 (§4.4.1). Plots of the variation of the normal and torque loads applied with time were thereafter made. .

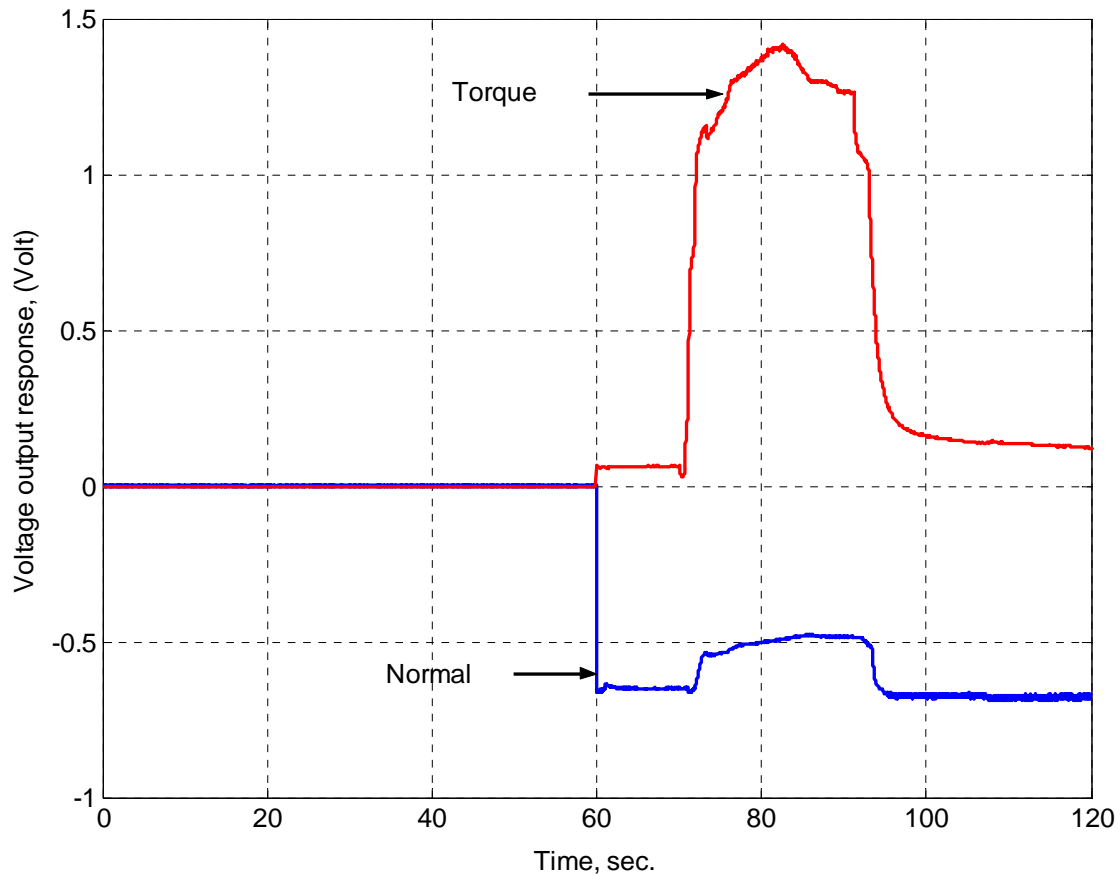


**Figure 4.20:** A typical plot of the output voltage responses of the shear apparatus showing the variation of the normal and torque loads with time

From Figure 4.20, prior to the initiation of the application of the shearing action by applying the torque load, the normal remains constant. However, with the application of the torque load, there occurred a slight decrease in the magnitude of the normal load. The fall in the normal load continues and only stops at the end of the application of the torque load. The decrease in the normal load voltage response was attributed to the sinkage of the head of the shear apparatus as it turns and penetrates the soil. It was also observed that greater fall in the normal load voltage response occurred if the application of the torque load was applied fast, i.e. in a short span of time. Therefore, all test runs

for the determination parameters of the shear strength and the soil-metal friction were performed at the slowest speed possible with the shearing apparatus.

On completion of the application of the torque load, the DAS was allowed to continue recording with the normal load maintained at the set level. During this session, the normal load returned to its original set value (from time of about 95 seconds to the end, Figure 4.20). With the normal load back to its set value, the shear apparatus tool-frame carrier was shifted laterally about 0.2 m from an already sheared spot and another test-run taken without altering the level of the normal load. This was repeated three times, i.e., three replications, after which the normal load was increased in steps of about 2kN and other test runs undertaken.